Macromolecules

Article

pubs.acs.org/Macromolecules

Hyperbranched Poly(aroxycarbonyltriazole)s: Metal-Free Click Polymerization, Light Refraction, Aggregation-Induced Emission, Explosive Detection, and Fluorescent Patterning

Hongkun Li,[†] Haiqiang Wu,[†] Engui Zhao,[‡] Jie Li,[‡] Jing Zhi Sun,[†] Anjun Qin,*[,†] and Ben Zhong Tang*[,†,‡,§]

[†]MOE Key Laboratory of Macromolecular Synthesis and Functionalization, Department of Polymer Science and Engineering, Zhejiang University, Hangzhou 310027, China

[‡]Department of Chemistry, Institute for Advanced Study, and Institute of Molecular Functional Materials, The Hong Kong University of Science & Technology, Clear Water Bay, Kowloon, Hong Kong, China

[§]Guangdong Innovative Research Team, State Key Laboratory of Luminescent Materials and Devices, South China University of Technology, Guangzhou 510640, China

Supporting Information

ABSTRACT: The metal-free click polymerization (MFCP) of azide and alkyne has become a powerful tool for the synthesis of functional polytriazoles. Among which, the MFCP of propiolate and azide has been used to prepare functional linear poly(aroxycarbonyltriazole)s (PACTs). Their hyperbranched analogues, however, have been rarely prepared. In this paper, hyperbranched PACTs with satisfactory molecular weights and high regioregularities were synthesized in high yields by the MFCP of tripropiolates (**1**) and tetraphenylethene (TPE)-containing diazide (**2**) under the optimized reaction conditions without protection from oxygen and moisture. The resultant polymers are soluble in common organic solvents and thermally stable, with 5% loss of their weights at temperatures higher than 330 °C. The polymers exhibit high refractive indices with low chromatic dispersion. Thanks to their contained TPE units, the polymers show the unique feature of aggregation-induced emission, and their aggregates can function as fluorescent sensors for the detection of explosives with the superamplification quenching effect. Furthermore, the polymers can be readily photo-cross-linked, yielding two-dimensional fluorescent patterns with high resolution.

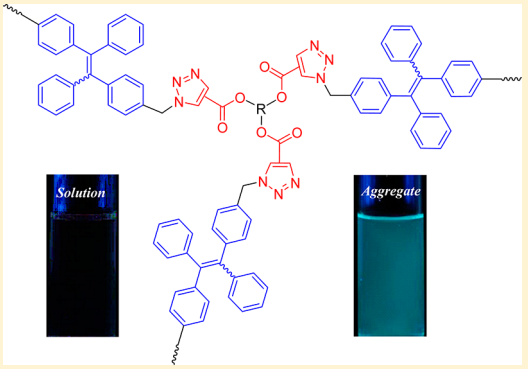

INTRODUCTION

Because of their unique architectures and properties, hyperbranched polymers have gained increasing research interests and are widely used in the areas of coatings, additives, drug delivery carriers, supramolecular chemistry, etc.[1,2] With persistent efforts of polymer chemists, various polymerization methods, such as polycondensation, polycyclotrimerization, and polycouplings, have been developed, and functional hyperbranched polymers have been prepared.[3] Generally, these polymerizations must be carried out under harsh reaction conditions, which greatly limit their applications. Thus, development of efficient polymerizations under mild reaction conditions becomes the key issue to expand the application of hyperbranched polymers.[4]

The azide−alkyne click polymerization, developed based on the well-known azide−alkyne click reactions and sharing their advantages of efficiency, mild reaction conditions, and function tolerance, etc.,[5] is an alternative efficient technique for the preparation of functional hyperbranched polymers.[6] Currently, the click polymerizations have mainly been mediated by metallic catalysts.[7,8] However, the catalyst residue is difficult to be completely removed from the resultant polymers and can cause cytotoxicity and deteriorate the photophysical properties of polymeric materials.[9] To circumvent this problem, the metal-free click polymerizations (MFCPs) of activated alkynes (aroylacetylenes/propiolates) and azide or activated azide and alkynes have been successfully established, and functional linear polytriazoles have been prepared under mild reaction conditions.[10]

Among these methods, the MFCP of propiolates and azides is promising to be utilized for the preparation of functional hyperbranched polytriazoles but rarely reported.[10c,d] One of the advantages of this polymerization is that the propiolate monomers could be facilely prepared from commercially available starting materials by one-step and one-pot reaction under ambient conditions. Furthermore, it could be carried out at a moderate temperature of 100 °C for 24 h in the mixed solvent of DMF and toluene even without protection from

Received: March 24, 2013
Revised: May 4, 2013
Published: May 16, 2013

oxygen and moisture, and soluble linear poly(aroxycarbonyltriazole)s (PACTs) with high molecular weights (M_w up to 23 500) and regioregularities (fraction of 1,4-disubstituted 1,2,3-triazole in PACTs up to ~90%) in excellent yields (up to ~99%) could be produced (Scheme 1).

Scheme 1. Synthesis of Poly(aroxycarbonyltriazole) (PACT) by Metal-Free Click Polymerization of Dipropiolate and Diazide

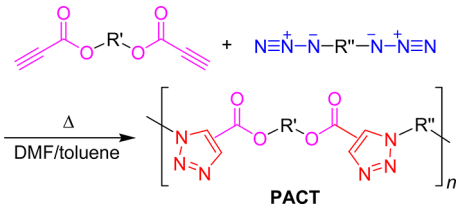

Encouraged by these exciting results and to extend the application of MFCP of propiolate and azide, in this paper, we synthesized the first example of soluble multifunctional hyperbranched PACTs (*hb*-PACTs) with high regioregularity by this method based on optimal reaction conditions. The *hb*-PACTs show high thermal stability and refractive indices and feature the aggregation-induced emission characteristics, and their aggregates could be used to detect explosive with superamplification quenching effect. Moreover, two-dimensional fluorescent patterns could readily be generated under UV irradiation.

EXPERIMENTAL SECTION

General Information. Tetrahydrofuran (THF) and toluene were distilled from sodium benzophenone ketyl in an atmosphere of nitrogen immediately prior to use. *N*,*N*-Dimethylformamide (DMF) was predried over calcium hydride, distilled under reduced pressure, and kept under nitrogen. Other solvents were purified by standard methods. Propiolic acid and 1,1,1-tris(hydroxymethyl)ethane were purchased from Alfa Aesar. Glycerin, *p*-toluenesulfonic acid, and picric acid were obtained from Sinopharm Group Chemical Reagent Co., Ltd. (China). All other chemicals were purchased from Acros or Aldrich and used as received without further purification.

Infrared (IR) spectra were taken on a Bruker Vector 22 spectrometer as thin films on KBr pellets. ^{1}H and ^{13}C NMR spectra were recorded on Bruker ADVANCE2B 400 NMR or Bruker DMX 500 NMR spectrometers in $CDCl_3$ or DMSO-d_6 using tetramethylsilane (TMS; $\delta = 0$) as internal reference. UV spectra were measured on a Varian VARY 100 Bio UV−vis spectrophotometer. Photoluminescence (PL) spectra were recorded on a RF-5301PC SERIES spectrofluorometer. Fluorescence quantum yields (Φ_F) were estimated using quinine sulfate in 0.1 N H_2SO_4 (Φ_F = 54.6%) as standard, and the absorbance of the solutions was kept around 0.05 to avoid internal filter effect. Element analysis was conducted on a Thermo Finnigan Flash EA1112 system. MALDI−TOF mass spectra were recorded on a GCT premier CAB048 mass spectrometer. Thermogravimetric analysis (TGA) measurements were carried out on a PerkinElmer TGA 7 under dry nitrogen at 20 °C/min. Refractive index (RI) values were determined on a Metricon Models 2010 and 2010/M prism coupler thin film thickness/refractive index measurement system. Relative weight-average (M_w) and number-average (M_n) molecular weights of the polymers and their polydispersity indices (PDI, M_w/M_n) were estimated by a Waters 1515 gel permeation chromatography (GPC) system equipped with an interferometric refractometer detector, using a set of monodispersed linear polystyrenes (PS) as calibration standards and THF as the eluents at a flow rate of 1.0 mL/min.

Monomer Preparation. The diazide of 1,2-bis[4-(azidomethyl)-phenyl]-1,2-diphenylethene (**2**) was prepared according to the experimental procedures described in our previous work.[11] The triynes of tripropiolates (**1**) were prepared by esterification of triols **4** with propiolic acid **3** in the presence of TsOH (Scheme 2). Detailed experimental procedures for the synthesis of 1,1,1-trimethylolethane tripropiolate (**1a**) are given below as an example.

Scheme 2. Synthetic Routes to Tripropiolates 1a and 1b

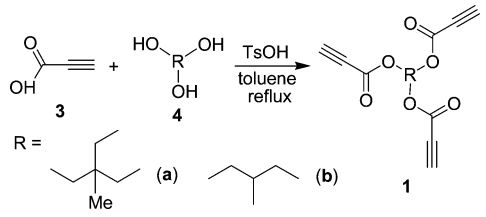

In a 250 mL round-bottom flask equipped with a Dean−Stark apparatus were added 2.47 g (20 mmol) of 1,1,1-tris(hydroxymethyl)-ethane (**4a**), 5.60 g (80 mmol) of propiolic acid (**3**), and 1.14 g (6 mmol) of TsOH in 100 mL of dry toluene. After refluxed for 48 h with constant removal of yielded water, the reaction mixture was concentrated, and the residues were dissolved in 100 mL of dichloromethane (DCM). The organic phase was washed with 5% aqueous $NaHCO_3$ solution (30 mL × 3) and water (50 mL × 1) and then dried over $MgSO_4$ overnight. After filtration and solvent evaporation, the crude product was purified by a silica gel column using petroleum ether/ethyl acetate (6:1, v/v) as eluent. 1,1,1-Trimethylolethane tripropiolate (**1a**) was obtained in 75.0% yield (4.14 g) as a white solid. IR (thin film), ν (cm^{-1}): 3274 (≡C−H stretching), 2936, 2122 (C≡C stretching), 1722 (C═O stretching), 1594, 1472, 1382, 1228, 995, 752, 698. ^{1}H NMR (400 MHz, DMSO-d_6), δ (TMS, ppm): 4.59 (s, 3H), 4.12 (s, 6H), 0.98 (s, 3H). ^{13}C NMR (100 MHz, DMSO-d_6), δ (ppm): 152.3, 75.9, 74.1, 67.2, 38.4, 16.5. Anal. Calcd for $C_{14}H_{12}O_6$: C, 60.87; H, 4.38. Found: C, 60.72; H, 4.39.

Propane-1,2,3-triyl tripropiolate (**1b**) was prepared with the similar procedures. Light-yellow viscous oil; yield 30.4%. IR (thin film), ν (cm^{-1}): 3280 (≡C−H stretching), 2971, 2123 (C≡C stretching), 1722 (C═O stretching), 1453, 1376, 1215, 1093, 1013, 950, 754, 682, 600. ^{1}H NMR (400 MHz, DMSO-d_6), δ (TMS, ppm): 5.40 (m, 1H), 4.71 (s, 1H), 4.66 (s, 2H), 4.46−4.36 (m, 4H). ^{13}C NMR (100 MHz, DMSO-d_6), δ (ppm): 151.7, 151.4, 76.8, 76.4, 73.6, 69.8, 62.9. HRMS (MALDI-TOF), m/z calculated for $C_{12}H_8O_6Na$ $[M + Na]^+$ = 271.0219; found = 271.0223.

Polymer Synthesis. All the polymerizations of tripropiolates and diazide were carried out in air, unless otherwise stated. Typical experimental procedures for the metal-free click polymerizations of **1** and **2** are shown below.

In a 15 mL Schlenk tube were placed 0.2 mmol of **1** and 0.3 mmol of **2**. Then, freshly distilled DMF (1.2 mL) was injected into the tube to dissolve the monomers. After stirring at 60 °C for 5 h, the reaction mixture was diluted with 10 mL of chloroform and added dropwise into 300 mL of hexane through a cotton filter under stirring. The precipitates were allowed to stand overnight and then collected by filtration. The polymer was washed with hexane and dried to a constant weight at ambient conditions.

Characterization Data of hb-PIa. The polymer was prepared by polymerization of 1,1,1-trimethylolethane tripropiolate (**1a**) and 1,2-bis[4-(azidomethyl)phenyl]-1,2-diphenylethene (**2**). White powder; 88.2% yield. M_w 7200; M_w/M_n 2.65 (GPC, determined in THF on the basis of PS calibration). Fraction of 1,4-disubstituted 1,2,3-triazoles in the polymer ($F_{1,4}$): 89.3%. IR (thin film), ν (cm^{-1}): 3268 (≡C−H stretching), 2960, 2918, 2115 (N_3 and C≡C stretching), 1727 (C═O stretching), 1545, 1467, 1389, 1213, 1046, 766, 699. ^{1}H NMR (400 MHz, DMSO-d_6), δ (TMS, ppm): 8.92, 8.64, 7.07, 6.93, 5.74, 5.55, 4.52, 4.31, 1.09. ^{13}C NMR (125 MHz, $CDCl_3$), δ (ppm): 160.3, 152.2, 144.4, 143.0, 140.6, 139.5, 133.6, 132.2, 131.3, 127.9, 126.6, 75.6, 74.1, 67.2, 54.1, 38.8, 16.7.

dx.doi.org/10.1021/ma400609m | *Macromolecules* 2013, 46, 3907−3914

Scheme 3. Synthesis of Hyperbranched Poly(aroxycarbonyltriazole)s *hb*-PIa and *hb*-PIb via Metal-Free Click Polymerizations of Tripropiolates 1 and Diazide 2

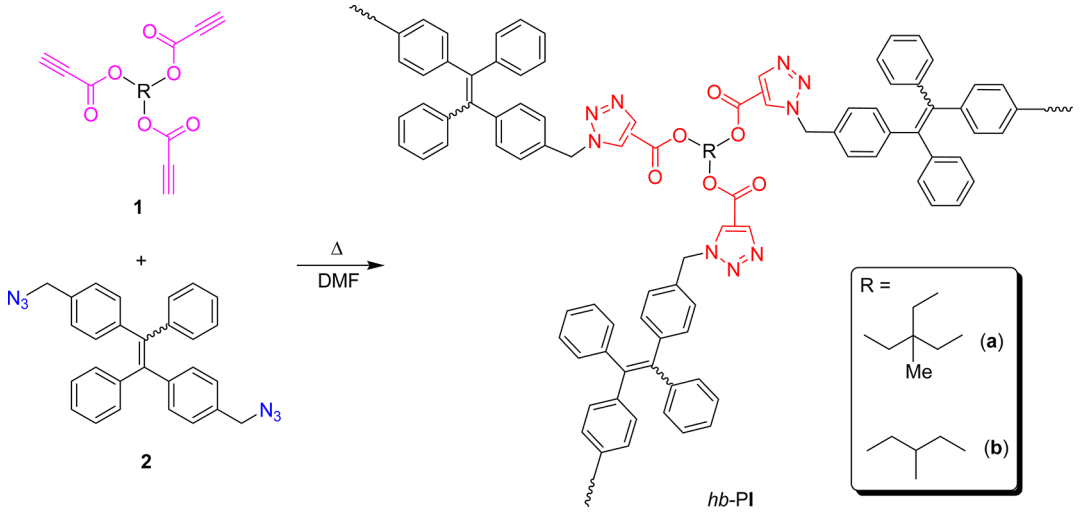

hb-PIb. The polymer was synthesized by the polymerization of propane-1,2,3-triyl tripropiolate (**1b**) and 1,2-bis[4-(azidomethyl)-phenyl]-1,2-diphenylethene (**2**). White powder; 91.6% yield. M_w 4400; M_w/M_n 2.21 (GPC, determined in THF on the basis of PS calibration). $F_{1,4}$: 82.6%. IR (thin film), ν (cm^{-1}): 3268 (≡C−H stretching), 3137, 2959, 2110 (N_3 and C≡C stretching), 1735 (C═O stretching), 1541, 1446, 1359, 1203, 1051, 849, 761, 703. ^{1}H NMR (400 MHz, DMSO-d_6), δ (TMS, ppm): 8.83, 8.68, 7.09, 6.93, 5.73, 5.54, 4.61, 4.35. ^{13}C NMR (125 MHz, $CDCl_3$), δ (ppm): 160.1, 151.9, 144.4, 142.9, 140.9, 139.4, 132.1, 131.0, 127.9, 126.7, 73.9, 69.8, 62.9, 54.2.

Fabrication of Fluorescent Patterns. Photo-cross-linking reactions of the polymer films were conducted in air at room temperature using the 365 nm UV light with an intensity of 18.5 mW/cm^2 as light source. The polymer films were prepared by spin-coating the polymer solution in 1,2-dichloroethane on silicon wafers and dried at room temperature overnight under reduced pressure. The photoresist patterns were generated using a copper photomask and taken on an Olympus BX41 fluorescent optical microscope with a 330−385 nm wide-band UV excitation.

RESULTS AND DISCUSSION

Monomer Synthesis. The tetraphenylethene (TPE)-containing diazide monomer **2** was prepared according to our reported procedures.[11] The tripropiolates **1** were facilely synthesized by a one-step and one-pot esterification of commercially available triols (**4**) and propiolic acid (**3**) in the presence of TsOH (Scheme 2). All the monomers were carefully purified and characterized by spectroscopic methods, from which satisfactory analysis data corresponding to their molecular structures were obtained (see Experimental Section for details).

Metal-Free Click Polymerization. In our previous work, we have established an efficient metal-free click polymerization (MFCP) of dipropiolate and diazide.[10c,d] These monomers could readily react at a moderate temperature of 100 °C, and functional linear PACTs with high molecular weights and regioregularities in excellent yields could be produced in a short reaction time. Encouraged by the high efficiency of this MFCP, in this paper, we tried to use it to prepare hyperbranched PACTs (*hb*-PACTs) (Scheme 3). Unfortunately, an insoluble gel was formed when tripropiolate **1a** and diazide **2** was reacted in DMF at 100 °C for 3.5−4 h. Thus, it is necessary to systematically optimize polymerization conditions for the preparation of soluble *hb*-PACTs.

We first investigated the effect of temperature on the polymerization of **1a** and **2** in DMF for 4 h with tripropiolate concentration of 0.167 M (Table 1). Similar to our first try, the gels were formed at 100 and 90 °C. The polymerizations carried out at 70 and 80 °C could produce soluble *hb*-PACTs with high M_w in high yields, but with very broad polydispersity indices (PDI > 6). Delightfully, soluble *hb*-PACT with the M_w and PDI values of 5200 and 2.07, respectively, could be obtained at lower reaction temperature of 60 °C. It is worth noting that the M_w values of hyperbranched polymers are normally underestimated as large as 7−30-fold by GPC using linear polystyrene as calibration.[12] Thus, 60 °C was selected as our optimized polymerization temperature.

Table 1. Effect of Temperature on the MFCP of 1a and 2[a]

entry	T (°C)	S^b	$M_w{}^c$	PDI^c	yield (%)
1	100	gel			
2	90	gel			
3	80	√	52 700	7.08	85.9
4	70	√	20 600	6.06	81.7
5	60	√	5 200	2.07	66.2

[a]Carried out in air for 4 h; [**1a**]/[**2**] = 2:3, [**1a**] = 0.167 M. [b]Solubility (S) tested in THF, DCM, chloroform, and DMF, etc.; √ = completely soluble. [c]M_w and PDI of polymer estimated by GPC in THF on the basis of a linear polystyrene calibration.

We then followed the time course of the polymerization of **1a** and **2** in DMF at 60 °C with former concentration of 0.167 M (Table 2). The M_w and PDI values of the polymer products generally increase with time except that for 8 h. The PDI values became broad after 5 h, and the yields decrease slightly after 6 h. We thus chose 5 h as our optimal reaction time when taking the M_w and PDI into account.

Finally, we studied the effect of the monomer concentration on the polymerization of **1a** with **2** in DMF at 60 °C for 5 h (Table 3). With increasing monomer concentration from 0.100 to 0.200 M, the yields of the *hb*-PACTs increased but with slight changes of their M_w and PDI. When considering the

dx.doi.org/10.1021/ma400609m | *Macromolecules* 2013, 46, 3907−3914

Table 2. Time Course on the MFCP of 1a and 2[a]

entry	t (h)	M_w[b]	PDI[b]	yield (%)
1	4	5 200	2.07	66.2
2	5	7 800	2.72	68.5
3	6	17 300	5.95	78.5
4	7	18 700	6.34	76.0
5	8	12 400	5.48	75.7

[a]Carried out in air at 60 °C; [**1a**]/[**2**] = 2:3, [**1a**] = 0.167 M. [b]M_w and PDI of polymer estimated by GPC in THF on the basis of a linear polystyrene calibration.

Table 3. Effect of Monomer Concentration on the MFCP of 1a and 2[a]

entry	[**1a**] (mol/L)	yield (%)	M_w[b]	PDI[b]
1	0.100	69.1	9200	4.00
2	0.120	71.3	8400	3.64
3	0.150	71.8	7800	3.56
4	0.167	76.6	7200	3.31
5	0.200	76.8	11 400	4.44

[a]Carried out in DMF at 60 °C in air for 5 h with [**1a**]/[**2**] = 2:3. [b]M_w and PDI of polymer estimated by GPC in THF on the basis of a linear polystyrene calibration.

yield, M_w, and PDI, we thus took 0.167 M as the optimized monomer concentration of **1a**.

Then, we used the optimized conditions to polymerize **1** and **2**, which propagated smoothly, and *hb*-P**Ia** and *hb*-P**Ib** with high molecular weights in high yields were obtained (Table 4).

Table 4. MFCPs of Tripropiolates 1 and Diazide 2[a]

entry	monomer	polymer	yield (%)	M_w[b]	PDI[b]	$F_{1,4}$[c] (%)
1	**1a** + **2**	*hb*-P**Ia**	88.2	7200	2.65	89.3
2[d]	**1a** + **2**	*hb*-P**Ia**	85.8	6100	2.44	88.5
3	**1b** + **2**	*hb*-P**Ib**	91.6	4400	2.21	90.9

[a]Carried out at 60 °C in air for 5 h; [**1**]/[**2**] = 2:3; [**1**] = 0.167 M. [b]M_w and PDI of polymer estimated by a GPC system equipped with an interferometric refractometer detector in THF on the basis of a linear polystyrene calibration. [c]Fraction of 1,4-disubstituted 1,2,3-triazoles in the products calculated from ^{1}H NMR spectra. [d]Carried out under nitrogen.

By comparing the polymerization results of **1a** and **2** in air and under nitrogen (cf. Table 4, entries 1 and 2), we can draw a conclusion that oxygen and moisture exert little effect on the polymerizations, which remarkably simplifies the reaction procedures.

Processability and Stability. All the freshly prepared hyperbranched polymers are completely soluble in commonly used organic solvents, such as THF, DCM, chloroform, 1,2-dichloroethane, and DMF. Furthermore, *hb*-P**Ia** and *hb*-P**Ib** can be readily fabricated into high quality thin solid films by spin-coating or solution casting process, which suggests that they are processable. They are also thermally stable. As can be seen from the TGA curves in Figure 1, the temperatures for 5% weight loss are higher than 330 °C under nitrogen, revealing their strong resistance to the thermolysis and oxidation at the elevated temperatures.

Structural Characterization. The polymers were characterized by spectroscopic methods, and satisfactory results corresponding to their expected molecular structures are

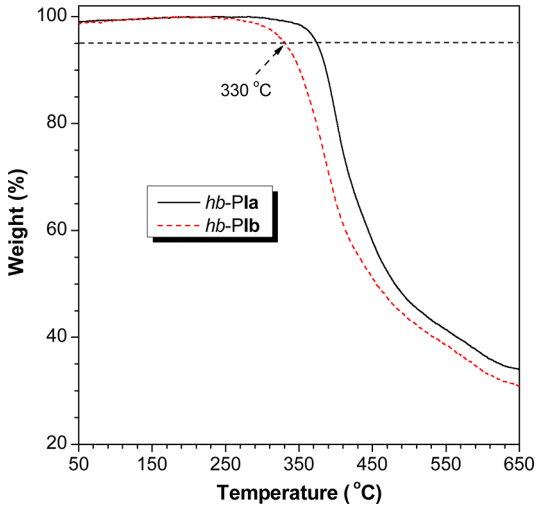

Figure 1. TGA thermograms of *hb*-P**Ia** and *hb*-P**Ib** recorded under nitrogen at a heating rate of 20 °C/min.

obtained (see Experimental Section and Supporting Information for details).

Examples of the IR spectra of *hb*-P**Ia** and its monomers are given in Figure 2. **1a** shows absorption bands at 3274 and 2122

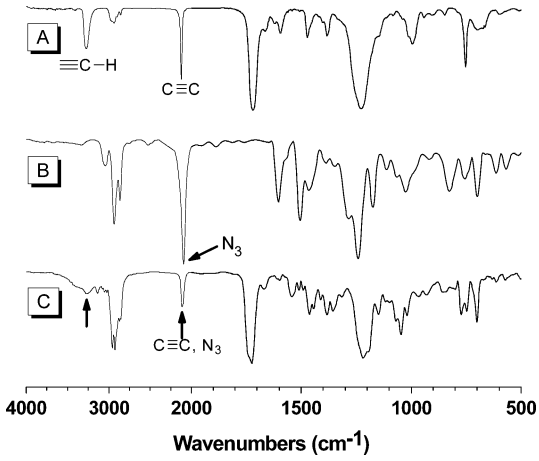

Figure 2. IR spectra of monomers **1a** (A) and **2** (B) and their polymer *hb*-P**Ia** (C).

cm^{-1} due to its ≡C−H and C≡C stretching vibrations, respectively. The strong absorption at 2101 cm^{-1} in the spectrum of **2** is associated with its azido group. All these absorption bands are still observed at similar wavenumbers but become weaker in the spectrum of *hb*-P**Ia**. This suggests that most of the ethynyl and azido groups of the monomers have been converted to the triazole rings of the polymer by the MFCP. The spectral profile of *hb*-P**Ib** is similar to that of *hb*-P**Ia** (Figure S1).

We have previously found that the ^{1}H NMR spectra of poly(aroyltriazole)s and PACTs measured in DMSO-d_6 have better resolution than in $CDCl_3$.[10f] Thus, we performed the ^{1}H NMR analysis of *hb*-P**I** in DMSO-d_6. The spectral profiles of *hb*-P**Ia** and *hb*-P**Ib** are similar, implying that the alkyl chain exerts little effect on the polymer structures (Figure 3 and Figure S2). Figure 3 shows the ^{1}H NMR spectra of polymer *hb*-P**Ia** and its monomers as an example. All resonance peaks of polymer and monomers are assignable. The resonances of the

dx.doi.org/10.1021/ma400609m | *Macromolecules* 2013, 46, 3907−3914

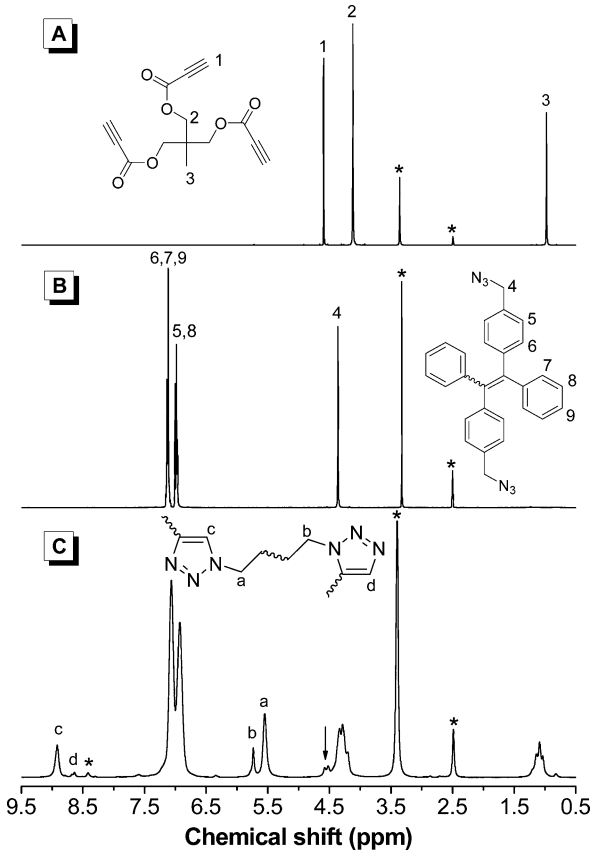

Figure 3. ^{1}H NMR spectra of monomer **1a** (A) and **2** (B) and their polymer *hb*-P**Ia** (C) in DMSO-d_6. The solvent and water peaks are marked with asterisks.

ethynyl protons of **1a** and the methylene protons adjacent to the azido groups of **2** at δ 4.59 and 4.37, respectively, become much weaker after polymerization. However, new peaks resonated at δ 8.92, 8.64, 5.74, and 5.55 are observed in the spectrum of *hb*-P**Ia**. The strong peaks at δ 8.92 (c) and 5.55 (a) are associated with the resonances of the protons in the triazole ring and its neighboring methylene group in the 1,4-isomeric units, while the weak signals at δ 8.64 (d) and 5.74 (b) stem from those in the 1,5-isomeric units. The results indicate that most of the ethynyl and azido groups of the monomers have been transformed into the triazole rings of the polymer by the MFCP, further confirming the conclusion drawn from the IR spectra analysis. The resonance peaks at δ 8.92 and 8.64 are well separated, which enables us to calculate the $F_{1,4}$ value from their integrals in the spectrum of *hb*-P**Ia**, which is as high as 89.3%. Similarly, the $F_{1,4}$ of *hb*-P**Ib** can also be calculated by this method, and an even higher value (90.9%) was deduced (Figure S2 and Table 4).

The ^{13}C NMR spectrum of *hb*-P**Ia** shows weak resonance peaks of acetylenic carbon atoms at δ 75.6 and 74.1 compared to those of its monomer. Furthermore, new peaks corresponding to the absorptions of the triazole carbons are observed at δ 140.6 and 139.5. These results again indicate that the ethynyl groups of **1a** and azides of **2** have been converted into the triazole rings in the polymer by the MFCP (Figure S3). Similar phenomena were observed in the ^{13}C NMR spectrum of *hb*-P**Ib** (Figure S4). Because of the poor resolution of related resonances in the ^{1}H and ^{13}C NMR spectra of *hb*-P**Ia** and *hb*-P**Ib**, the important parameter of degree of branching is hardly assessed.

Optical Transparency and Light Refractivity. Polymers intended for photonic applications should have a high degree of optical clarity.[13] *hb*-P**Ia** and *hb*-P**Ib** absorb no light at wavelengths longer than 390 nm in chloroform solutions (Figure 4), indicating that they are highly transparent in the visible spectral region. This excellent optical transparency is due to their contained alkyl and ester repeating units, which breaks the electronic communications and decreases the effective conjugation of the polymer chains. The high optical transparency makes the *hb*-PACTs promising for photonic applications.[14]

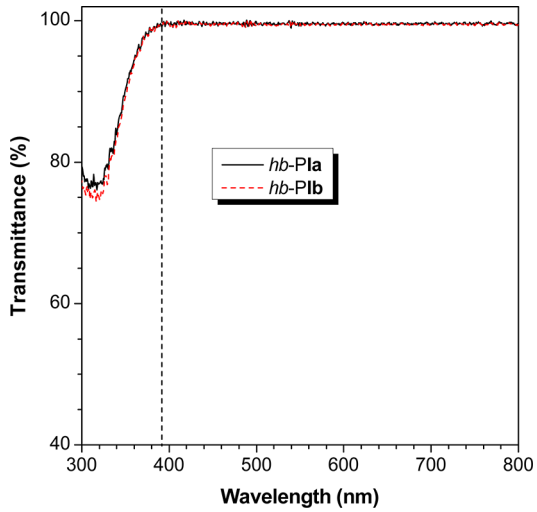

Figure 4. Transmission spectra of chloroform solutions of *hb*-P**Ia** and *hb*-P**Ib**. Polymer concentration: 10 μM.

Since the *hb*-P**I** contains polarized triazole rings and ester groups, they are expected to show high refractive index (RI) values (n).[15] Wavelength-dependent refractivity measurements confirm that *hb*-P**Ia** and *hb*-P**Ib** possess high RI values of 1.614−1.586 and 1.622−1.589 in the wavelength region of 600−1550 nm, respectively (Figure 5). It is worth noting that these values are higher than those of the commercially

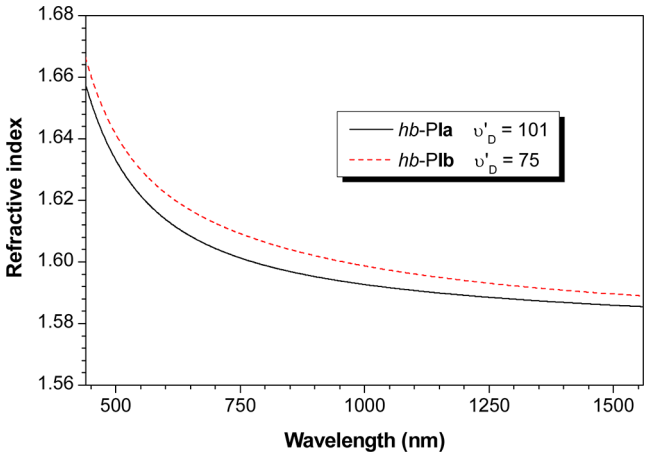

Figure 5. Light refraction spectra of thin solid films of *hb*-P**Ia** and *hb*-P**Ib** and variation of modified Abbé number (υ'_D) with polymer structures.

dx.doi.org/10.1021/ma400609m | *Macromolecules* 2013, 46, 3907−3914

important optical plastics such as poly(methyl methacrylate) (n = 1.489) and polycarbonate (n = 1.582). In addition, the development of polymeric materials with low chromatic dispersion is of importance for practical applications. The Abbé number (υ_D) of a material is a measure of the variation or dispersion in its RI values with wavelength. To evaluate the application potential of an optical material, it is suggested to use a modified Abbé number (υ'_D) calculated by its RI values at the nonabsorbing wavelengths of 1064, 1319, and 1550 nm.[16] The first two wavelengths are chosen in view of the practical interest of commercial laser wavelengths, while the last one is the wavelength for telecommunication. The modified Abbé number is defined as eq 1:

$$\upsilon'_D = \frac{n_{1319} - 1}{n_{1064} - n_{1550}} \quad (1)$$

where n_{1319}, n_{1064}, and n_{1550} are the RI values at 1319, 1064, and 1550 nm, respectively.

The υ'_D values for *hb*-P**Ia** and *hb*-P**Ib** were calculated to be 101 and 75, which are much higher than those for the conjugated polymers with absorptions in the visible spectral region ($\upsilon'_D \approx 10-40$). Since optical dispersion is inversely proportional to the Abbé number, the *hb*-P**Ia** and *hb*-P**Ib** thus have very low optical dispersion. Thus, this MFCP paves a facile and effective way to prepare photonic hyperbranched polytriazoles with high refractive index values and low chromatic dispersion.

Aggregation-Induced Emission. As shown in Scheme 3, *hb*-P**Ia** and *hb*-P**Ib** were synthesized by MFCP of triynes **1** and TPE-containing diazide **2**. Previously, we have found that TPE is a typical luminogen exhibiting aggregation-induced emission (AIE) characteristic, which refers to a unique phenomenon that a series of propeller-shaped molecules are nonemissive when molecularly dissolved but emit intensely when aggregated or fabricated in solid films, and the restriction of intramolecular rotation (RIR) has been rationalized as the mechanism.[17,18] The AIE-active TPE-containing linear polytriazoles have been prepared by the Cu(I)-catalyzed and metal-free click polymerizations and been well-investigated.[19] The TPE-containing hyperbranched polytriazoles showing AIE feature are, however, rarely reported.[7a,b]

According to our previous work,[7b] the TPE-containing hyperbranched polymers possessing flexible alkyl chains can be endowed with the AIE feature. *hb*-P**Ia** and *hb*-P**Ib** also contain such chains and are expected to preserve the AIE features. We thus investigated their emission behaviors in the THF/water mixtures with different water fraction (f_w). Figure 6A shows the PL spectra of *hb*-P**Ia** as an example. When excited with the maximum absorption at 318 nm, the PL curve of a diluted THF solution of *hb*-P**Ia** is almost a flat line parallel to the abscissa; in other words, the polymer is virtually nonluminescent. On the contrary, the fluorescence emission is progressively intensified with its spectral profile remaining unchanged upon gradual addition of water into its THF solution. The similar emission behaviors of *hb*-P**Ib** were also observed in its PL spectra (Figure S5). Evidently, *hb*-P**Ia** and *hb*-P**Ib** are AIE-active.

The AIE characteristics of *hb*-P**Ia** and *hb*-P**Ib** were further verified by the variations of their fluorescence quantum yields (Φ_F) in the solution and aggregate states. In pure THF, *hb*-P**Ia** and *hb*-P**Ib** both show negligibly small Φ_F values of 0.20 and 0.23%, respectively (Figure 6B). The Φ_F values of them increase progressively with gradual addition of water and reach

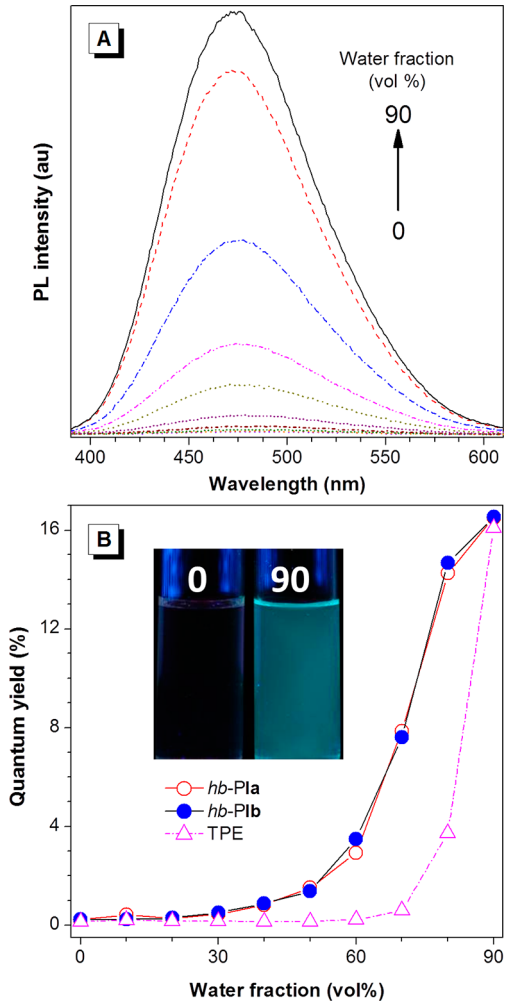

Figure 6. (A) PL spectra of *hb*-P**Ia** in THF and THF/water mixtures. Concentration: 10 μM; λ_{ex}: 318 nm. (B) Variation in the quantum yields (Φ_F) of *hb*-P**Ia**, *hb*-P**Ib** and TPE in THF/water mixtures with different water fractions. The Φ_F values were estimated using quinine sulfate in 0.1 M H_2SO_4 (Φ_F = 54.6%) as standard. Inset in panel B: solutions of *hb*-P**Ia** in pure THF and a THF/water mixture with 90% water; photographs taken under illumination of a hand-held UV lamp.

the highest values of 16.51 and 16.53% at the f_w of 90%, which are 82- and 72-fold higher than those in pure solvents, respectively. Furthermore, these Φ_F values of polymers are close to that of TPE under the same experimental conditions at the f_w of 90%, suggesting that the emission behavior of TPE was preserved in the polymers after MFCP.

The AIE features of *hb*-P**Ia** and *hb*-P**Ib** could be attributed to their intrinsic architectures. According to the RIR mechanism, even after the TPE units have been incorporated into the polymer branches, their peripheral phenyl rings can still rotate freely in the solution state, making the polymers nonemissive. In the aggregate state, however, the intramolecular rotation is restricted, which effectively blocks the nonradiative energy dissipation channels of the polymers and turns on their light emission.

Explosive Detection. Prompted by the AIE characteristics of the *hb*-P**Ia** and *hb*-P**Ib**, we utilized them as fluorescent sensors for the explosive detection, which is important in the fields of homeland security and antiterrorism.[20] Because 2,4,6-trinitrophenol (picric acid, PA) is commercially available, we then use it as a model explosive among the nitroaromatic

dx.doi.org/10.1021/ma400609m | *Macromolecules* 2013, 46, 3907−3914

compounds. The aggregates of polymers in THF/water mixtures with f_w of 90% were utilized as the fluorescent sensors due to their highest emission intensities. For comparison, the nanoaggregate of TPE was also used to detect PA.

Figure 7A shows the PL behaviors of *hb*-P**Ia** upon addition of PA as an example. With gradual addition of PA, the PL

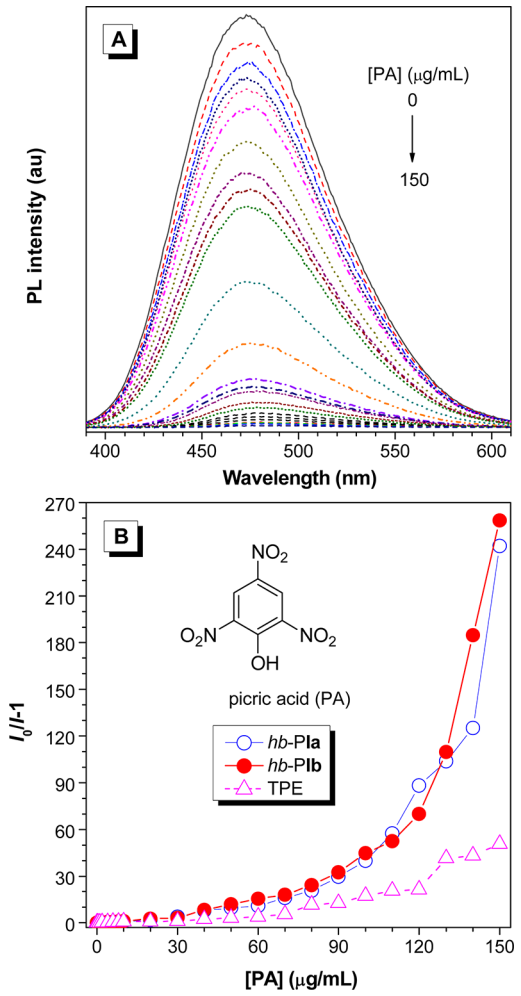

Figure 7. (A) PL spectra of the *hb*-P**Ia** in THF/water mixtures (f_w: 90%) containing different amounts of picric acid (PA). Concentration: 10 μM. λ_{ex}: 318 nm. (B) Stern–Volmer plots of $I_0/I - 1$ of *hb*-P**Ia**, *hb*-P**Ib**, and TPE versus PA concentration, where I = peak intensity and I_0 = peak intensity at [PA] = 0 μg/mL. Inset: the chemical structure of PA.

intensities of *hb*-P**Ia** aggregates progressively decreased but with no change in the spectral profiles. Similar PL behaviors are observed for *hb*-P**Ib** aggregates, and their detection limits for PA could be as low as 1 μg/mL. The aggregates of TPE can also be used to detect PA and the Stern–Volmer plot is almost linear with PA concentration, giving a quenching constant of 13 400 M^{-1}, whereas the plots of *hb*-P**Ia** and *hb*-P**Ib** show linear correlation with quenching constants of 19 500 and 26 700 M^{-1}, respectively, when the PA concentrations are lower than 20 μg/mL (Figure 7B). Afterward, the curves bend upward, which shows a unique superamplification quenching effect, which are similar to our previous research.[21]

Fluorescence Patterning. Thanks to the AIE feature, film-forming ability of *hb*-P**Ia** and *hb*-P**Ib**, and the remaining unreacted ethynyl and azide groups on their peripheries, which can be cross-linked upon UV irradiation, the polymer films could be employed to generate fluorescent patterns. When thin solid films of *hb*-P**Ia** and *hb*-P**Ib** on silicon wafers were irradiated under a UV light through copper photomasks, the exposed region was cross-linked and bleached probably through a nitrene-mediated photolysis mechanism,[7c] whereas the unexposed area remains emissive. Two-dimensional fluorescent patterns with sharp line edges were thus readily generated without going through the development processes (Figure 8).

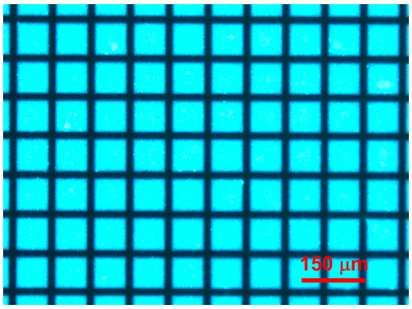

Figure 8. Two-dimensional fluorescent pattern of *hb*-P**Ia**. The photograph was taken under UV irradiation.

CONCLUSION

In summary, we have successfully prepared functional *hb*-PACTs by the efficient metal-free click polymerization of tripropiolates and TPE-containing diazide. Through investigation of the reaction conditions, we found that *hb*-PACTs with satisfactory molecular weights and high regioregularities ($F_{1,4}$ up to 90.9%) could be produced in high yields (up to 91.6%) after the monomers reacted in DMF at 60 °C for 5 h without protection from oxygen and moisture. The resultant *hb*-PACTs are completely soluble in organic solvents and thermally stable. Furthermore, they possess good film-forming ability and display high refractive indices with low chromatic dispersions. Thanks to the AIE feature of their contained TPE units, the *hb*-PACTs are also AIE-active, and their aggregates can work as fluorescent chemosensors for the detection of explosives with superamplification quenching effect. The multifunctional *hb*-PACTs make them promising candidates for high-tech applications.

ASSOCIATED CONTENT

Supporting Information

IR and ^{1}H NMR spectra of *hb*-P**Ib** and their monomers; ^{13}C NMR spectra of *hb*-P**Ia** and *hb*-P**Ib** and their monomers; PL spectra of *hb*-P**Ib** in THF/water mixtures. This material is available free of charge via the Internet at http://pubs.acs.org.

AUTHOR INFORMATION

Corresponding Author

*E-mail: qinaj@zju.edu.cn (A.J.Q.); tangbenz@ust.hk (B.Z.T).

Notes

The authors declare no competing financial interest.

ACKNOWLEDGMENTS

This work was partially supported by the National Science Foundation of China (21222402, 21174120 and 20974098); the key project of the Ministry of Science and Technology of

China (2013CB834702 and 2009CB623605), and the Research Grants Council of Hong Kong (603509, HKUST2/CRF/10, 604711 and N-HKUST620/11).

REFERENCES

(1) (a) Khandare, J.; Calderón, M.; Dagia, N. M.; Haag, R. *Chem. Soc. Rev.* **2012**, *41*, 2824. (b) Gao, H.; Yorifuji, D.; Wakita, J.; Jiang, Z.; Ando, S. *Polymer* **2010**, *51*, 3173. (c) Zhou, Y. F.; Huang, W.; Liu, J. Y.; Zhu, X. Y.; Yan, D. Y. *Adv. Mater.* **2010**, *22*, 4567. (d) Voit, B. I.; Lederer, A. *Chem. Rev.* **2009**, *109*, 5924. (e) Pu, K. Y.; Li, K.; Shi, J. B.; Liu, B. *Chem. Mater.* **2009**, *21*, 3816. (f) Gao, C.; Yan, D. *Prog. Polym. Sci.* **2004**, *29*, 183. (g) Mori, H.; Muller, A. H. E. *Top. Curr. Chem.* **2003**, *228*, 1. (h) Jikei, M.; Kakimoto, M. *Prog. Polym. Sci.* **2001**, *26*, 1233. (i) Hecht, S.; Fréchet, J. M. J. *Angew. Chem., Int. Ed.* **2001**, *40*, 74. (j) Hawker, C. J. *Adv. Polym. Sci.* **1999**, *147*, 113. (k) Yates, C. R.; Hayes, W. *Eur. Polym. J.* **2004**, *40*, 1257.

(2) (a) Liu, J.; Lam, J. W. Y.; Tang, B. Z. *Chem. Rev.* **2009**, *109*, 5799. (b) Häußler, M.; Qin, A.; Tang, B. Z. *Polymer* **2007**, *48*, 6181. (c) Häußler, M.; Tang, B. Z. *Adv. Polym. Sci.* **2007**, *209*, 1.

(3) (a) Hu, Y.; Chen, L.; Guo, Z.; Nagai, A.; Jiang, D. *J. Am. Chem. Soc.* **2011**, *133*, 17622. (b) Wu, W.; Ye, S.; Huang, L.; Xiao, L.; Fu, Y.; Huang, Q.; Yu, G.; Liu, Y.; Qin, J.; Li, Q.; Li, Z. *J. Mater. Chem.* **2012**, *22*, 6374. (c) Liu, J.; Zhong, Y.; Lam, J. W. Y.; Lu, P.; Hong, Y.; Yu, Y.; Yue, Y.; Faisal, M.; Sung, H. H. Y.; Williams, I. D.; Wong, K. S.; Tang, B. Z. *Macromolecules* **2010**, *43*, 4921. (d) Hu, R.; Lam, J. W. Y.; Liu, J.; Sung, H. H. Y.; Williams, I. D.; Yue, Z.; Wong, K. S.; Yuen, M. M. F.; Tang, B. Z. *Polym. Chem.* **2012**, *3*, 1481. (e) Yuan, W.; Hu, R.; Lam, J. W. Y.; Xie, N.; Jim, C. K. W.; Tang, B. Z. *Chem.—Eur. J.* **2012**, *18*, 2847. (f) Shu, W.; Guan, C.; Guo, W.; Wang, C.; Shen, Y. *J. Mater. Chem.* **2012**, *22*, 3075.

(4) (a) Han, J.; Zhu, D.; Gao, C. *Polym. Chem.* **2013**, *4*, 542. (b) Qin, A. J.; Lam, J. W. Y.; Dong, H. C.; Lu, W. X.; Jim, C. K. W.; Dong, Y. Q.; Häussler, M.; Sung, H. H. Y.; Williams, I. D.; Wong, G. K. L.; Tang, B. Z. *Macromolecules* **2007**, *40*, 4879.

(5) (a) Rostovtsev, V. V.; Green, L. G.; Fokin, V. V.; Sharpless, K. B. *Angew. Chem., Int. Ed.* **2002**, *41*, 2596. (b) Tornøe, C. W.; Christensen, C.; Meldal, M. *J. Org. Chem.* **2002**, *67*, 3057. (c) Lo, C. N.; Hsu, C. S. *J. Polym. Sci., Part A: Polym. Chem.* **2011**, *49*, 3355. (d) Park, J. S.; Kim, Y. H.; Song, M.; Kim, C. H.; Karim, Md. A.; Lee, J. W.; Gal, Y. S.; Kumar, P.; Kang, S. W.; Jin, S. H. *Macromol. Chem. Phys.* **2011**, *211*, 2464. (e) Schwartz, E.; Breitenkamp, K.; Fokin, V. V. *Macromolecules* **2011**, *44*, 4735.

(6) (a) Li, H.; Sun, J. Z.; Qin, A.; Tang, B. Z. *Chin. J. Polym. Sci.* **2012**, *30*, 1. (b) Qin, A. J.; Lam, J. W. Y.; Tang, B. Z. *Chem. Soc. Rev.* **2010**, *39*, 2522. (c) Qin, A. J.; Lam, J. W. Y.; Tang, B. Z. *Macromolecules* **2010**, *43*, 8693. (d) Sumerlin, B. S.; Vogt, A. P. *Macromolecules* **2010**, *43*, 1. (e) Binder, W. H.; Sachsenhofer, R. *Macromol. Rapid Commun.* **2007**, *28*, 15.

(7) (a) Wang, J.; Mei, J.; Zhao, E.; Song, Z.; Qin, A.; Sun, J. Z.; Tang, B. Z. *Macromolecules* **2012**, *45*, 7692. (b) Wang, J.; Mei, J.; Yuan, W.; Lu, P.; Qin, A.; Sun, J.; Ma, Y.; Tang, B. Z. *J. Mater. Chem.* **2011**, *21*, 4056. (c) Qin, A.; Lam, J. W. Y.; Jim, C. K. W.; Zhang, L.; Yan, J.; Häussler, M.; Liu, J.; Dong, Y.; Liang, D.; Chen, E.; Jia, G.; Tang, B. Z. *Macromolecules* **2008**, *41*, 3808.

(8) (a) Li, D. Z.; Wang, X.; Jia, Y. T.; Wang, A. Q.; Wu, Y. G. *Chin. J. Chem.* **2012**, *30*, 861. (b) Pandey, S.; Mishra, S. P.; Kolli, B.; Kanai, T.; Samui, A. B. *J. Polym. Sci., Part A: Polym. Chem.* **2012**, *50*, 2659. (c) Wu, W. B.; Ye, C.; Yu, G.; Liu, Y. Q.; Qin, J. G.; Li, Z. *Chem.—Eur. J.* **2012**, *18*, 4426. (d) Plietzsch, O.; Schilling, C. I.; Grab, T.; Grage, S. L.; Ulrich, A. S.; Comotti, A.; Sozzani, P.; Muller, T.; Brase, S. *New J. Chem.* **2011**, *35*, 1577. (e) Katritzky, A. R.; Song, Y. M.; Sakhuja, R.; Gyanda, R.; Meher, N. K.; Wang, L.; Duran, R. S.; Ciaramitaro, D. A.; Bedford, C. D. *J. Polym Sci, Part A: Polym. Chem.* **2009**, *47*, 3748. (f) Katritzky, A. R.; Meher, N. K.; Hanci, S.; Gyanda, R.; Tala, S. R.; Mathai, S.; Duran, R. S.; Bernard, S.; Sabri, F.; Singh, S. K.; Doskocz, J.; Ciaramitaro, D. A. *J. Polym. Sci, Part A: Polym. Chem.* **2008**, *46*, 238. (g) Xie, J. D.; Hu, L. H.; Shi, W. F.; Deng, X. X.; Cao, Z. Q.; Shen, Q. S. *J. Polym. Sci., Part B: Polym. Phys.* **2008**, *46*, 1140. (h) Scheel, A. J.; Komber, H.; Voit, B. *Macromol. Rapid Commun.* **2004**, *25*, 1175.

(9) (a) Zhang, J.; Zhang, K.; Huang, X.; Cai, W.; Zhou, C.; Liu, S.; Huang, F.; Cao, Y. *J. Mater. Chem.* **2012**, *22*, 12759. (b) Lou, X.; Ou, D.; Li, Q.; Li, Z. *Chem. Commun.* **2012**, *48*, 8462. (c) Wang, Q.; Chan, T. R.; Hilgraf, R.; Fokin, V. V.; Sharpless, K. B.; Finn, M. G. *J. Am. Chem. Soc.* **2003**, *125*, 3192. (d) Dong, H. C.; Zheng, R. H.; Lam, J. W. Y.; Häussler, M.; Qin, A. J.; Tang, B. Z. *Macromolecules* **2005**, *38*, 6382.

(10) (a) Wei, Q.; Wang, J.; Shen, X.; Zhang, X.; Sun, J. Z.; Qin, A.; Tang, B. Z. *Sci. Rep.* **2013**, *3*, 1093. (b) Wang, Q.; Li, H. K.; Wei, Q.; Sun, J. Z.; Wang, J.; Zhang, X. A.; Qin, A. J.; Tang, B. Z. *Polym. Chem.* **2013**, *4*, 1396. (c) Li, H.; Wang, J.; Hu, R.; Sun, J. Z.; Qin, A. J.; Tang, B. Z. *Polym. Chem.* **2012**, *3*, 1075. (d) Li, H.; Mei, J.; Wang, J.; Zhang, S.; Zhao, Q.; Wei, Q.; Qin, A. J.; Sun, J. Z.; Tang, B. Z. *Sci. China Chem.* **2011**, *54*, 611. (e) Qin, A. J.; Tang, L.; Lam, J. W. Y.; Jim, C. K. W.; Yu, Y.; Zhao, H.; Sun, J. Z.; Tang, B. Z. *Adv. Funct. Mater.* **2009**, *19*, 1891. (f) Qin, A. J.; Jim, C. K. W.; Lu, W. X.; Lam, J. W. Y.; Häussler, M.; Dong, Y. Q.; Sung, H. Y.; Williams, I. D.; Wong, G. K. L.; Tang, B. Z. *Macromolecules* **2007**, *40*, 2308.

(11) Qin, A.; Tang, L.; Lam, J. W. Y.; Jim, C. K.; Zhao, H.; Sun, J.; Tang, B. Z. *Macromolecules* **2009**, *42*, 1421.

(12) (a) Uhrich, K. E.; Hawker, C. J.; Fréchet, J. M. J.; Turner, S. R. *Macromolecules* **1992**, *25*, 4583. (b) Muchtar, Z.; Schappacher, M.; Deffieux, A. *Macromolecules* **2001**, *34*, 7595. (c) Grayson, S. M.; Fréchet, J. M. J. *Macromolecules* **2001**, *34*, 6542. (d) Xu, K.; Peng, H.; Sun, Q.; Dong, Y.; Salhi, F.; Luo, J.; Chen, J.; Huang, Y.; Xu, Z.; Tang, B. Z. *Macromolecules* **2002**, *35*, 5821.

(13) (a) Yoon, J.; Mathers, R. T.; Coates, G. W.; Thomas, E. L. *Macromolecules* **2006**, *39*, 1913. (b) Fukukawa, K.; Shibasaki, Y.; Ueda, M. *Macromolecules* **2004**, *37*, 8256.

(14) (a) Liu, J.; Lam, J. W. Y.; Jim, C. K. W.; Ng, J. C. Y.; Shi, J.; Su, H.; Yeung, K. F.; Hong, Y.; Mahtab, F.; Yu, Y.; Wong, K. S.; Tang, B. Z. *Macromolecules* **2011**, *44*, 68. (b) Jim, C. K. W.; Qin, A. J.; Lam, J. W. Y.; Liu, J. Z.; Häussler, M.; Yuen, M. M. F.; Kim, J. K.; Ng, K. M.; Tang, B. Z. *Macromolecules* **2009**, *42*, 4099.

(15) (a) Nakagawa, Y.; Suzuki, Y.; Higashihara, T.; Ando, S.; Ueda, M. *Macromolecules* **2011**, *44*, 9180. (b) Bhagat, S. D.; Chatterjee, J.; Chen, B.; Stiegman, A. E. *Macromolecules* **2012**, *45*, 1174.

(16) (a) Yang, C. J.; Jenekhe, S. A. *Chem. Mater.* **1994**, *6*, 196. (b) Yang, C. J.; Jenekhe, S. A. *Chem. Mater.* **1995**, *7*, 1276.

(17) (a) Luo, J. D.; Xie, Z. L.; Lam, J. W. Y.; Cheng, L.; Chen, H. Y.; Qiu, C. F.; Kwok, H. S.; Zhan, X. W.; Liu, Y. Q.; Zhu, D. B.; Tang, B. Z. *Chem. Commun.* **2001**, 1740. (b) Hong, Y. N.; Lam, J. W. Y.; Tang, B. Z. *Chem. Commun.* **2009**, 4332. (c) Hong, Y. N.; Lam, J. W. Y.; Tang, B. Z. *Chem. Soc. Rev.* **2011**, *40*, 5361.

(18) (a) Chen, J.; Law, C. W.; Lam, J. W. Y.; Dong, Y.; Lo, S. M. F.; Williams, I. D.; Zhu, D.; Tang, B. Z. *Chem. Mater.* **2003**, *15*, 1535. (b) Qin, A.; Lam, J. W. Y.; Mahtab, F.; Jim, C. K. W.; Tang, L.; Sun, J.; Sung, H. H. Y.; Williams, I. D.; Tang, B. Z. *Appl. Phys. Lett.* **2009**, *94*, 253308. (d) Qian, L.; Zhi, J.; Tong, B.; Yang, F.; Zhao, W.; Dong, Y. *Prog. Chem.* **2008**, *20*, 673. (e) Li, Z.; Dong, Y.; Mi, B.; Tang, Y.; Haussler, M.; Tong, H.; Dong, Y.; Lam, J. W. Y.; Ren, Y.; Sung, H. H. Y.; Wong, K. S.; Gao, P.; Williams, I. D.; Kwok, H. S.; Tang, B. Z. *J. Phys. Chem. B* **2005**, *109*, 10061.

(19) (a) Hu, R.; Lam, J. W. Y.; Tang, B. Z. *Macromol. Chem. Phys.* **2013**, *214*, 175. (b) Qin, A. J.; Lam, J. W. Y.; Tang, B. Z. *Prog. Polym. Sci.* **2012**, *37*, 182.

(20) Salinas, Y.; Martinez-Manez, R.; Marcos, M. D.; Sancenon, F.; Costero, A. M.; parra, M.; Gil, S. *Chem. Soc. Rev.* **2012**, *41*, 1261.

(21) (a) Liu, J.; Zhong, Y.; Lu, P.; Hong, Y.; Lam, J. W. Y.; Faisal, M.; Yu, Y.; Wong, K. S.; Tang, B. Z. *Polym. Chem.* **2010**, *1*, 426. (b) An, Z. F.; Zheng, C.; Chen, R. F.; Yin, J.; Xiao, J. J.; Shi, H. F.; Tao, Y.; Qian, Y.; Huang, W. *Chem.—Eur. J.* **2012**, *18*, 15655.